

# Enhanced dynamic properties of Ge-on-Si mode-evolution waveguide photodetectors

A. Palmieri\*, A. Shafiee\*, M. G. C. Alasio\*, A. Tibaldi\*<sup>†</sup>, G. Ghione\*, F. Bertazzi\*<sup>†</sup>, M. Goano\*<sup>†</sup>, M. Vallone\*

\* Dipartimento di Elettronica e Telecomunicazioni, Politecnico di Torino, corso Duca degli Abruzzi 24, 10129 Torino, Italy

<sup>†</sup> IEIIT-CNR, corso Duca degli Abruzzi 24, 10129 Torino, Italy

E-mail: michele.goano@polito.it

**Abstract**—This work discusses coupled three-dimensional electromagnetic and electrical simulations of a Ge-on-Si waveguide photodetector where light is fed through a lateral waveguide. The numerical results show that this coupling solution leads to more uniform photon and carrier distributions along the Ge absorber compared to a conventional butt-coupled detector, allowing a broader electrooptical bandwidth for high input power levels in good agreement with available experimental measurements.

## I. INTRODUCTION

The computer-aided design and optimization of next-generation Ge-on-Si waveguide photodetectors (WPDs) for silicon photonics [1] requires a three-dimensional multiphysics picture describing the interplay between optical field propagation and transport of photogenerated carriers. Evanescent coupling of light in the Ge absorber by means of a lateral waveguide (mode-evolution coupling, MEC) has been proposed as a promising alternative to conventional butt-coupled (BC) WPD structures to minimize the impact of screening effects related to high-carrier injection [2]. This work presents a comparative simulation study of the BC and MEC WPDs proposed in [2], demonstrating the ability of a multiphysics approach to reproduce the broader electrooptical bandwidth at high optical power levels allowed by the MEC solution.

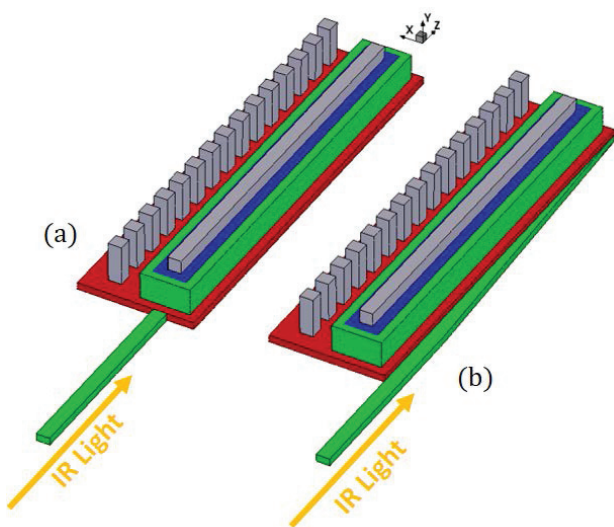


Fig. 1. Perspective view of a BC (a) and MEC (b) detector.

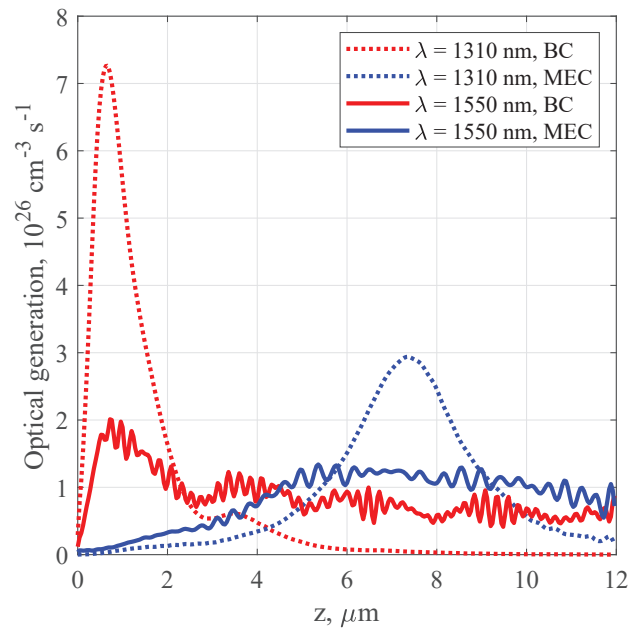


Fig. 2. Optical generation rate in Ge averaged over the WPD cross-section as a function of  $z$ , for the BC and the MEC detector.

## II. PHOTODETECTOR STRUCTURE AND MODELING APPROACH

Fig. 1 shows the photodetector structures proposed in [2]: on top of a  $\text{SiO}_2$  substrate, an intrinsic Ge region 800 nm thick and  $12 \mu\text{m}$  long lies over a thin Si base; both metallic contacts are in tungsten. In the simulated structures a steep, error-function-shaped  $p$ -doping profile with peak  $N_A = 10^{19} \text{cm}^{-3}$  is assumed at the W/Ge interface, and the Si base has a uniform  $n$ -type doping  $N_D = 10^{18} \text{cm}^{-3}$ . The transport properties of Ge, including doping-dependent mobilities and high-field carrier velocity saturation, are described as in [3], while the optical properties of Ge are taken from [4].

Electrical simulations are performed in the drift-diffusion framework taking into account Fermi-Dirac statistics and incomplete dopant ionization, and considering Shockley-Read-Hall (SRH), radiative and Auger processes as generation-recombination terms.

Geometry and doping of the detector are defined with the Sentaurus TCAD suite by Synopsys [5], also used to

perform the electrical simulations. The electromagnetic problem is solved by a full-wave approach with Synopsys RSoft FullWAVE [6] according to the Finite Difference Time Domain (FDTD) method [7]. Multiphysics coupling is achieved through a one-way linking strategy where the optical generation rate distribution  $G_{opt}(x, y, z)$ , obtained from the time-averaged Poynting vector, is used as a source term in the drift-diffusion continuity equations.

### III. RESULTS, COMMENTS AND CONCLUSIONS

Fig. 2 shows, as a function of the longitudinal coordinate  $z$ , the optical generation rate integrated over the Ge cross-section at 1.31 and 1.55  $\mu\text{m}$ . Independently from the input wavelength, we can observe a different behavior of the BC and MEC WPDs: the first is characterized by an intense absorption in the first few micrometers along  $z$ , whereas the photogeneration is much more uniformly distributed along the MEC device. This results in an important effect on the dynamic properties of the two detectors, as shown in the electrooptical frequency response reported in Fig. 3. For 200  $\mu\text{W}$  of input optical power, at 1.55  $\mu\text{m}$  the BC and MEC responses are overlapped and in good agreement with experimental values from [2], but at 1.31  $\mu\text{m}$  the BC bandwidth is  $\approx 6$  GHz narrower than the MEC one (see the inset in Fig. 3). In fact, at 1.31  $\mu\text{m}$  the Ge absorption is higher, and the BC WPD is affected by a stronger screening of the electric field induced by the  $G_{opt}$  peak; hence the photogenerated carriers are extracted less efficiently [8] and the bandwidth is reduced. The better performance of the MEC WPD can be also appreciated in Fig. 4, which shows the electrooptical cutoff frequency for increasing optical power: for its maximum considered value (2 mW), the MEC WPD has a bandwidth  $\approx 11$  GHz broader than the BC device. Further improvements should be obtained by exploring the MEC parameter space with the help of multiphysics simulation.

### IV. ACKNOWLEDGEMENTS

This work was supported in part by Cisco Systems, Inc., under the Sponsored Research Agreement TOSCA-2.

### REFERENCES

- [1] A. H. Atabaki, S. Moazeni, F. Pavanello, H. Gevorgyan, J. Notaros, L. Alloatti, M. T. Wade, C. Sun, S. A. Kruger, H. Meng, K. Al Qubaisi, I. Wang, B. Zhang, A. Khilo, C. V. Baiocco, M. A. Popovic, V. M. Stojanovic, and R. J. Ram, "Integrating photonics with silicon nanoelectronics for the next generation of systems on a chip," *Nature*, vol. 556, pp. 349–354, 2018.
- [2] M. J. Byrd, E. Timurdogan, Z. Su, C. V. Poulton, N. M. Fahrenkopf, G. Leake, D. D. Coolbaugh, and M. R. Watts, "Mode-evolution-based coupler for high saturation power Ge-on-Si photodetectors," *Opt. Lett.*, vol. 42, no. 4, pp. 851–854, Feb. 2017.
- [3] A. Palmieri, M. Vallone, M. Calciati, A. Tibaldi, F. Bertazzi, G. Ghione, and M. Goano, "Heterostructure modeling considerations for Ge-on-Si waveguide photodetectors," *Opt. Quantum Electron.*, vol. 50, no. 2, p. 71, Feb. 2018.
- [4] V. Sorianello, L. Colace, N. Armani, F. Rossi, C. Ferrari, L. Lazzarini, and G. Assanto, "Low-temperature germanium thin films on silicon," *Opt. Mater. Expr.*, vol. 1, no. 5, pp. 856–865, Sept. 2011.
- [5] *Sentaurus Device User Guide. Version N-2017.09*, Synopsys, Inc., Mountain View, CA, Sept. 2017.
- [6] *RSoft FullWAVE User Guide, v2017.03*, Synopsys, Inc., Inc., Optical Solutions Group, Ossining, NY, 2017.

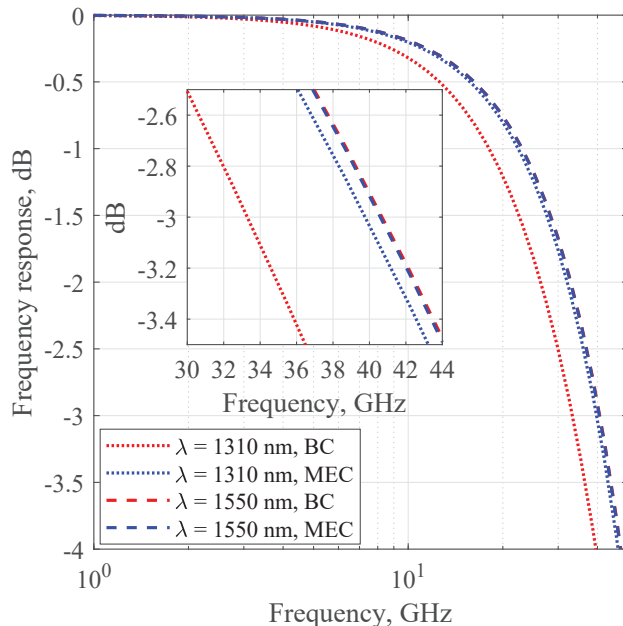


Fig. 3. Electrooptical frequency response for a BC and a MEC detector, for 200  $\mu\text{W}$  of input optical power at a reverse bias of 1 V.

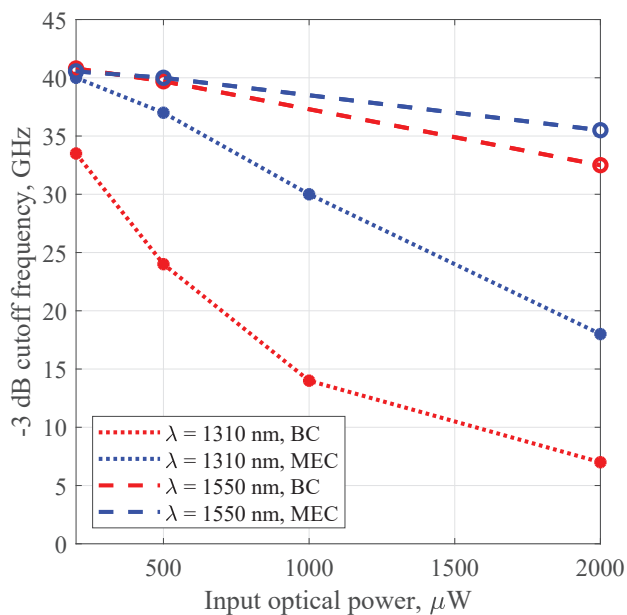


Fig. 4. Electrooptical cutoff frequency as a function of the input optical power for the BC and MEC detector.

- [7] J.-P. Berenger, "A perfectly matched layer for the absorption of electromagnetic waves," *J. Comp. Phys.*, vol. 114, no. 2, pp. 185–200, 1994.
- [8] M. Vallone, A. Palmieri, M. Calciati, F. Bertazzi, M. Goano, G. Ghione, and F. Forghieri, "3D physics-based modelling of Ge-on-Si waveguide  $p$ - $i$ - $n$  photodetectors," in *17th International Conference on Numerical Simulation of Optoelectronic Devices (NUSOD 2017)*, Copenhagen, Denmark, July 2017, pp. 207–208.